

## Corrosion behavior of as-cast $\text{Mg}_{68}\text{Zn}_{28}\text{Y}_4$ alloy with *I*-phase

SHI Fei(史 菲)<sup>1,2</sup>, YU Yuan-chun(于元春)<sup>3</sup>, GUO Xue-feng(郭学锋)<sup>2</sup>,  
ZHANG Zhong-ming(张忠明)<sup>2</sup>, LI Ying-ying(李瑛颖)<sup>1</sup>

1. School of Materials Science and Engineering, Harbin Institute of Technology(Weihai), Weihai 264209, China;
2. School of Materials Science and Engineering, Xi'an University of Technology, Xi'an 710048, China;
3. Department of Applied Chemistry, Harbin Institute of Technology(Weihai), Weihai 264209, China

Received 1 July 2008; accepted 17 December 2008

**Abstract:**  $\text{Mg}_{68}\text{Zn}_{28}\text{Y}_4$  alloys with stable icosahedral quasicrystals ( $\text{Zn}_{60}\text{Mg}_{30}\text{Y}_{10}$ ) were prepared by cast method. By simulating the environment of ocean, the alloy was eroded in 3.5% (mass fraction) NaCl for 2, 4 and 30 h. The microstructures of the samples and eroded alloys were analyzed by OM and SEM. The compositions and the quasiperiodic structures were identified respectively by EDS and TEM. And the corrosion potential and corrosion current density before and after immersion were measured by potentiodynamic polarization measurements in 3.5% NaCl. The results show that *I*-phases grow in the mode of conglomeration, piling and transfixion. The  $\text{Mg}_7\text{Zn}_3$  matrix and  $\alpha(\text{Mg})$  solid solution are eroded badly, while *W*-phase is eroded partially. At the same time, the *I*-phases exhibit excellent corrosion resistance property. The resistance to corrosion of  $\text{Mg}_{68}\text{Zn}_{28}\text{Y}_4$  alloy is improved by increasing exposed *I*-phases. With adding element Y to  $\text{Mg}_{68}\text{Zn}_{32}$  alloy, the corrosion current is decreased by one order of magnitude. And after the immersion of as-cast  $\text{Mg}_{68}\text{Zn}_{28}\text{Y}_4$  alloy for 30 h, the corrosion current density is reduced by two orders of magnitude compared with that of uneroded  $\text{Mg}_{68}\text{Zn}_{32}$  alloy.

**Key words:** as-cast magnesium alloy; corrosion resistance; icosahedral quasicrystal; Mg-Zn-Y alloy

## 1 Introduction

Magnesium alloy is a lightweight engineering material with a variety of excellent properties such as high specific strength, low density, good electromagnetic shielding characteristics and castability, high heat conductivity, damping capacity and machability. As a result of these advantages, magnesium alloys have been found widespread applications from portable micro-electronics to automobiles and aircrafts[1–6]. However, despite improving the mechanical performance, it is essential to overcome the high susceptibility of magnesium alloys to corrosion which occurs either in acid, neutral or alkali solutions, even in pure water[7]. Today, the existing methods to improve the corrosion resistance of magnesium alloys are divided into three categories[8]. The first one is improving the purity of magnesium alloys or adding metal elements to the alloys thus forming new functional materials; the second one

lies in enlarging the solid-saturation and refining grains by rapid solidification; and surface treatment is the third method.

In this work, adding yttrium element to the  $\text{Mg}_{68}\text{Zn}_{32}$  alloys so that the  $\text{Mg}_{68}\text{Zn}_{28}\text{Y}_4$  ternary alloys with icosahedral quasicrystal phase (*I*-phase)[9–12] were prepared by as-cast method. That is to say, the melted alloys are autogenetic composite materials of magnesium alloys with icosahedral quasicrystals. The corrosion behaviors under the simulated ocean condition were studied. And the corrosion resistances of magnesium alloys were tested.

## 2 Experimental

Alloys with compositions of  $\text{Mg}_{68}\text{Zn}_{32}$  and  $\text{Mg}_{68}\text{Zn}_{28}\text{Y}_4$  were prepared from the master alloy Mg-25%Y (mass fraction), high purity Mg (99.9%, mass fraction) and Zn(99.9%, mass fraction) by melting in graphite crucibles in 3 kW electric resistance furnace.

**Foundation item:** Project(50271054) supported by the National Natural Science Foundation of China; Project(2002E110) supported by the Natural Science Foundation of Shaanxi Province, China; Project supported by the Scientific Research Foundation of the Education Department of Shaanxi Province for the Returned Overseas Chinese Scholars

**Corresponding author:** SHI Fei; Tel: +86-631-5687880; E-mail: shifeixian@163.com

DOI: 10.1016/S1003-6326(08)60412-4

The mixed salt of 50% NaCl and 50% KCl was melted to prevent evaporation of Zn and oxidation during casting. After the solution treatment, the solidified alloys were cast on the cast-iron board. Finally, the specimen thickness was about 2 mm.

At room temperature, the alloy specimens were eroded for 0, 2, 4 and 30 h in 3.5% NaCl solution. After immersion, the samples were cleaned by 15%  $\text{CrO}_3$ +1%  $\text{AgNO}_3$  mixture solution, then wiped with alcohol, dried in air and further put in desiccator for 24 h before the tests.

The microstructures and *I*-phase of uneroded and eroded alloys were characterized by optical microscope and scanning electron microscope (TESCAN VEGA II / SBH). The corresponding compositions were analyzed by energy dispersive X-ray analysis (EDAX GENESIS 2048). And the icosahedral quasicrystal structure was identified by transmission electron microscope (JEM-200CX). The potentiodynamic polarization measurements were performed with a conventional three-electrode cell in 3.5% NaCl at room temperature. A platinum electrode of 1  $\text{cm}^2$  was used as an auxiliary electrode.  $\text{Mg}_{68}\text{Zn}_{32}$  and  $\text{Mg}_{68}\text{Zn}_{28}\text{Y}_4$  alloys were used as the working electrodes.

### 3 Results

#### 3.1 Microstructures of original sample

Fig.1 shows the SEM images of the as-cast  $\text{Mg}_{68}\text{Zn}_{28}\text{Y}_4$  alloy at room temperature. It is obvious that the bright white quasicrystals (*I*-phases) existing as the primary phases of the alloy distribute on the matrix. When being cooled on the cast-iron surface (left in map) and in air (right in map), the grains of *I*-phases are finer and more. However, in the center, the amount of *I*-phases is decreased, and only a few *I*-phases have conditions to grow up, as shown in Fig.1(a). The EDS analysis for the gray phase shows that there are elements such as Mg and Zn. The contents of Mg and Zn are 68.97% and 31.03%, respectively. Therefore,  $\text{Mg}_7\text{Zn}_3$  is likely to be the matrix phase in the as-cast  $\text{Mg}_{68}\text{Zn}_{28}\text{Y}_4$  alloy. The black dendrite containing 99.28% Mg with a few of Zn and O can be figured as  $\alpha(\text{Mg})$  solid solution. The bright white icosahedral quasicrystals appearing in small pentagon, hexagon and petal-shape are enwrapped in *W*-phase ( $\text{Mg}_3\text{Zn}_3\text{Y}_2$ ), which are shown in Fig.1(b). The compositions of *I*-phase are 61.19% Zn, 28.58% Mg and 10.23% Y (molar fraction), which are the closest to  $\text{Zn}_{60}\text{Mg}_{30}\text{Y}_{10}$  (*I*-phase) of the ternary Mg-Zn-Y system. The TEM morphologies and the quasicrystalline state of  $\text{Mg}_{68}\text{Zn}_{28}\text{Y}_4$  alloy were obtained by SHI et al[13]. Selected area electron diffraction patterns of these phases with special patterns, pentagonal, hexagonal or petaling are taken on the five-fold symmetry structure, thereby

proving the characteristics of quasi-periodically atomic ordering. Thus, it is validated that the as-cast microstructures of  $\text{Mg}_{68}\text{Zn}_{28}\text{Y}_4$  alloy mainly contain the gray  $\text{Mg}_7\text{Zn}_3$  matrix,  $\alpha(\text{Mg})$  solid solution,  $\text{Mg}_3\text{Zn}_3\text{Y}_2$  (*W*-phase) and  $\text{Zn}_{60}\text{Mg}_{30}\text{Y}_{10}$  (*I*-phase) by SEM, EDS and TEM analyses.

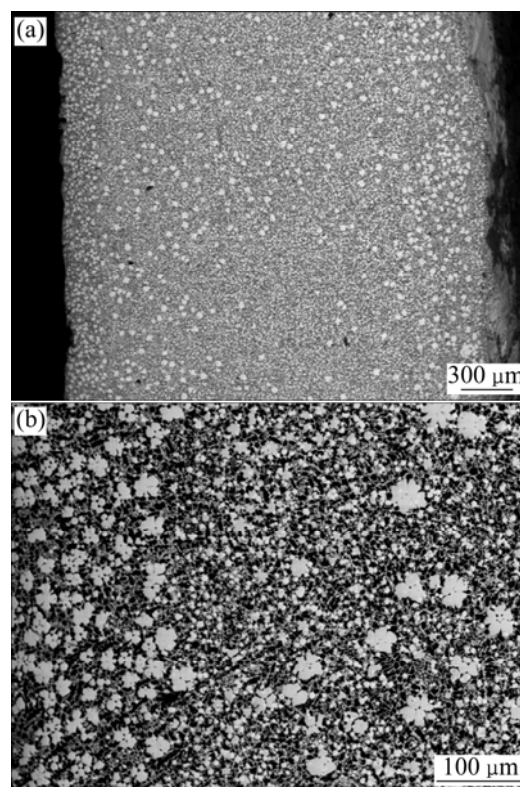


**Fig.1** As-cast microstructures of  $\text{Mg}_{68}\text{Zn}_{28}\text{Y}_4$  alloy cooling on cast-iron surface: (a) *I*-Phase; (b) *W*-phase

#### 3.2 Corrosion resistance

It could be observed from samples immersed in the 3.5% NaCl solutions that there are volumes of the gases bubbled up from the surface of samples. When it is immersed for 1 h, the corrosion solution gradually appears in green color, with a dram of white powder produced. The as-cast microstructures eroded for 2 h is shown in Fig.2(a). The  $\text{Mg}_7\text{Zn}_3$  matrix and  $\alpha(\text{Mg})$  solid solution in surface layer are eroded partly, meanwhile *W*-phase surrounding the *I*-phase starts to erode gradually from the exterior to the quasicrystal phases, thereby exposing the quasicrystal phases embedded in the matrix. The *I*-phases grow with the conglomeration, which is shown with arrow.

The SEM image of sample immersed for 4 h is shown in Fig.2(b). The pitting corrosion is expanded to the general corrosion due to the poor corrosion resistance of  $\text{Mg}_7\text{Zn}_3$  matrix. The corrosion pits are left by the mass corrosion of the surface layer of  $\alpha(\text{Mg})$  solid solution. The more erosion the matrix phase is,  $\alpha(\text{Mg})$  solid solution and *W*-phase experience, the more the deep

layer *I*-phases expose. This gives rise to the amounts of the *I*-phases per unit area. *W*-phases are eroded more severely by immersion in the corrosion solutions and dissolve from the alloy, which leads to the quasicrystal phase growing from the conglomeration to the dispersion. Moreover, the limitations of quasicrystal structures cause the phenomenon of desquamating along cleavage planes. From the macroscopic observation, the amount of overflowing gas decreases gradually, whereas that of the white solid powder increases with the color of the corrosion solution changing from green to white.

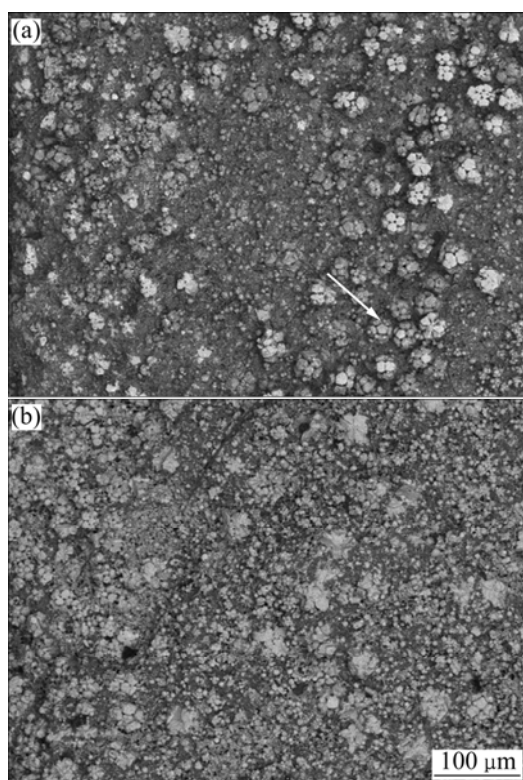


**Fig.2** SEM micrographs of as-cast  $\text{Mg}_{68}\text{Zn}_{28}\text{Y}_4$  alloy eroded in 3.5% NaCl for different time: (a) 2 h; (b) 4 h

After samples are eroded in 3.5% NaCl solution for 30 h, the corrosion solution becomes white and produces a great deal of white solid powder sediment. It can be concluded from Fig.3(a) that the  $\alpha(\text{Mg})$  solid solution eroded in the corrosion solution disappears and a few  $\text{Mg}_7\text{Zn}_3$  matrix are left, while part of *W*-phase still exists. The amount of the *I*-phase per unit area increases as this corrosion process goes on; furthermore, the five-petaling or six-petaling *I*-phase begins to be eroded from the first petal to the body. Figs.3(b) and (c) show distinctly that the *I*-phase grows with the mode of conglomeration, piling and transfixion. At the same time, the icosahedral prismatical quasicrystal grains with hexagonal end face can be seen apparently. EDS analyses show that there are 57.83% Zn, 30.20% Mg and 11.52% Y (molar fraction) in the icosahedral grains.

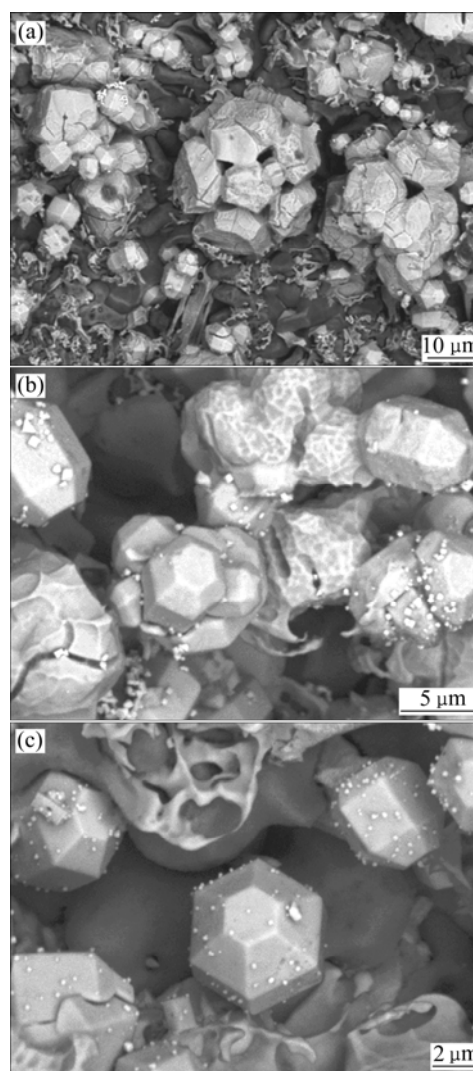


**Fig.3** As-cast microstructures of  $\text{Mg}_{68}\text{Zn}_{28}\text{Y}_4$  eroded for 30 h in 3.5% NaCl: (a) Disappearing of  $\alpha(\text{Mg})$  solid solution; (b) and (c) *I*-phase growth

### 3.3 Electrochemical properties

The corrosion potential and corrosion current density of  $\text{Mg}_{68}\text{Zn}_{32}$  and  $\text{Mg}_{68}\text{Zn}_{28}\text{Y}_4$  alloys determined by extrapolating the anodic-cathodic Tafel lines are listed in Table 1.

**Table 1** Corrosion potential and corrosion current density of  $\text{Mg}_{68}\text{Zn}_{32}$  and  $\text{Mg}_{68}\text{Zn}_{28}\text{Y}_4$  alloys before and after immersion

Sample	Condition	$\phi_{\text{corr}}/\text{V}$	$J_{\text{corr}}/(\text{mA}\cdot\text{cm}^{-2})$
$\text{Mg}_{68}\text{Zn}_{32}$	Without immersion	-1.50	4.780
	Before immersion	-1.44	0.492
$\text{Mg}_{68}\text{Zn}_{28}\text{Y}_4$	After immersion for 30 h	-1.35	0.060

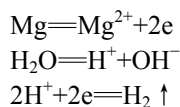
By comparing the corrosion potential of  $\text{Mg}_{68}\text{Zn}_{32}$  and  $\text{Mg}_{68}\text{Zn}_{28}\text{Y}_4$  alloys before immersion, it can be found that the corrosion potential of  $\text{Mg}_{68}\text{Zn}_{28}\text{Y}_4$  alloy is a little

positive than that of  $\text{Mg}_{68}\text{Zn}_{32}$  alloy. The corrosion current density of  $\text{Mg}_{68}\text{Zn}_{28}\text{Y}_4$  alloy is markedly less than that of  $\text{Mg}_{68}\text{Zn}_{32}$  alloy by one order of magnitude, indicating the remarkable enhancement of corrosion protection ability of  $\text{Mg}_{68}\text{Zn}_{28}\text{Y}_4$  ternary alloy than that of  $\text{Mg}_{68}\text{Zn}_{32}$  alloy by adding a small amount of Y element. For  $\text{Mg}_{68}\text{Zn}_{28}\text{Y}_4$  alloy, the corrosion potential after immersion for 30 h is more positive than that before immersion. And the corrosion current density after immersion for 30 h is also markedly less than that before immersion, reduced by one order of magnitude. The results illuminate that the corrosion protection ability of alloy eroded for 30 h is enhanced superiorly. With increasing the imposed *I*-phases in corrosion process, large numbers of fine and dispersed *I*-phases in the surface layer prevent interior alloy from corrosion, thus, the corrosion protection ability of magnesium alloys is enhanced obviously.

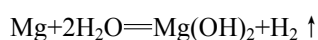
#### 4 Discussion

According to the as-cast microstructures and Mg-Zn-Y ternary alloy phase diagram, the  $\alpha(\text{Mg})$  solid solution is born in advance to the process of solidification of  $\text{Mg}_{68}\text{Zn}_{28}\text{Y}_4$  alloy. *W*-phases are created under the effect of solute solidification and segregation. With decreasing the temperature of fused mass, a peritectic reaction occurs at approximately 900 K:  $L + \text{Mg}_3\text{Zn}_3\text{Y}_2(W) \rightarrow \text{Zn}_{60}\text{Mg}_{30}\text{Y}_{10}(I)$ , then icosahedral quasicrystal is created, including nucleation and growth of first order reaction.

Being immersed in the air or solution, magnesium alloys produce an oxide film with porosity characteristic which is lack of excellent protection for magnesium alloys[14]. Hydrogen damage is the main corrosion of magnesium alloys, and alloys are melted rapidly by pitting corrosion or comprehensive corrosion[15]. In corrosive solution, the different potentials of phases lead to many micro galvanic cells, whose susceptibility is dominated by  $\alpha(\text{Mg})$  phase. The reactions occurred in the corrosion processing of  $\text{Mg}_{68}\text{Zn}_{28}\text{Y}_4$  alloys are as follows:



The main equation is



According to the equation, the overflowing gas from the surface of sample is  $\text{H}_2$ , whereas in the corrosion process, the sediment of white solid powder is  $\text{Mg}(\text{OH})_2$ . The amount of overflowing  $\text{H}_2$  decreases gradually with the continuation of corrosion process due to the dissolution of Mg, as well as the  $\text{Mg}(\text{OH})_2$  that

clings on the surface of specimens thus impeding the reactions for  $\text{H}^+$  to obtain the electrons in solutions. In addition, the element yttrium in  $\text{Mg}_{68}\text{Zn}_{28}\text{Y}_4$  alloys produces  $\text{Y}_2\text{O}_3$  that distributes in the oxide films of the specimens surface incontinuously. Because of its low chemical activity, the susceptibility to corrosion medium of  $\text{Y}_2\text{O}_3$  is reduced, therefore strengthening the protection function of alloy oxide films.

The eroded process of  $\text{Mg}_{68}\text{Zn}_{28}\text{Y}_4$  alloy with *I*-phase in 3.5% NaCl solution is shown in Fig.4. Fig.4(a) displays the uneroded state of alloy. In the corrosion process, the metal on the surface is eroded in advance by pitting corrosion, with the releasing of  $\text{H}_2$  as well as  $\text{Mg}(\text{OH})_2$  sedimentations, by the continuous exposure of *I*-phase in the corrosion solution, as shown in Figs.4(b) and (c). The excellent corrosion resistance of *I*-phase reduces the corrosion rate of alloy. As this process goes on, the amount of *I*-phases per unit area increases sharply, as shown in Fig.4(d), which enhances the general corrosion resistance of samples.

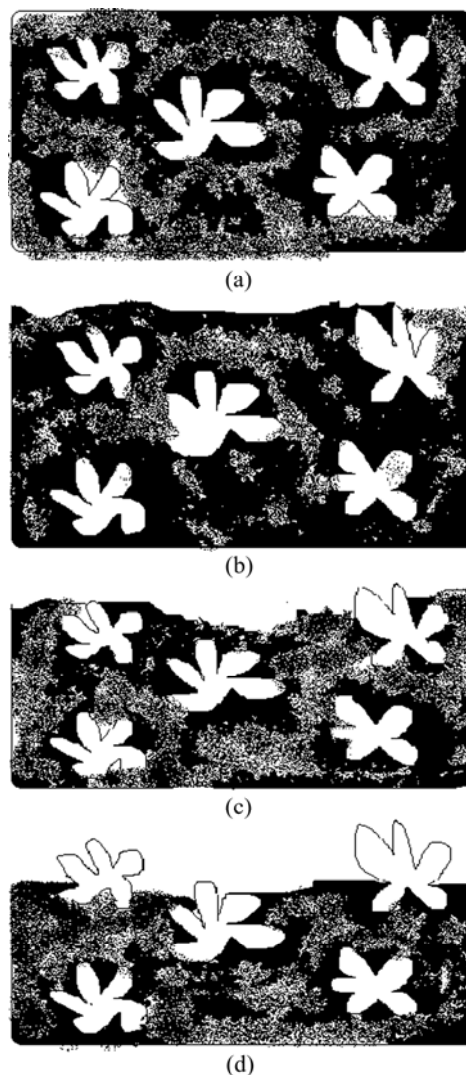


**Fig.4** Schematic drawing of as-cast  $\text{Mg}_{68}\text{Zn}_{28}\text{Y}_4$  alloy eroded in 3.5% NaCl

The primary strengthening phase in the  $\text{Mg}_{68}\text{Zn}_{28}\text{Y}_4$  alloy is icosahedral one. If this autogenetic composite material of magnesium alloy with icosahedral quasicrystals can be used as a surface treating material, depending on excellent corrosion resistance and connection with magnesium alloys, the corrosion resistance and the application fields of magnesium alloys will be improved greatly.

## 5 Conclusions

1) The  $\text{Mg}_{68}\text{Zn}_{28}\text{Y}_4$  alloy is eroded in 3.5% NaCl solution. In this process,  $\text{H}_2$  and  $\text{Mg}(\text{OH})_2$  are produced. Meanwhile, the amount of *I*-phases per unit area is increased.

2) Icosahedral quasicrystal phases grow in the mode of conglomeration, piling and transfixion. The *I*-phase with inerratic hexagon can be seen apparently.

3) Tafel curves reveal that the corrosion resistance of the  $\text{Mg}_{68}\text{Zn}_{28}\text{Y}_4$  alloy is improved significantly after 30 h of immersion in 3.5% solution with the corrosion potential of  $-1.35$  V and corrosion current density of  $0.060$  mA/cm<sup>2</sup>.

4) The autogenetic composite materials of magnesium alloys with icosahedral quasicrystals can be used as surface treating materials to protect the base metal from corrosion, thus improving the corrosion resistance of alloys.

## References

- [1] LINDSTROM R, JOHANSSON L G, THOMPSON G E. Corrosion of magnesium in humid air [J]. Corrosion Science, 2004, 46: 1141–1158.
- [2] GRAY J E, LUAN B. Protective coatings on magnesium and its alloys—A critical review [J]. Journal of Alloys and Compounds, 2002, 336: 88–113.
- [3] KUBOTA K, MABUCH M, HIGASHI K. Review—Processing and mechanical properties of fine-grained magnesium alloys [J]. Journal of Materials Science, 1999, 34: 2255–2262.
- [4] MORDIKE B L, EBERT T. Magnesium: Properties- applications-potential [J]. Mater Sci Eng A, 2001, 302: 37–45.
- [5] SINGH A, WATANABE M, KATO A, TSAI A P. Quasicrystal strengthened Mg-Zn-Y alloys by extrusion [J]. Scripta Mater, 2003, 49: 417–422.
- [6] LAMBRI O A, RIEHEMANN W, TROJANOVA Z. Mechanical spectroscopy of commercial AZ91 magnesium alloy [J]. Scripta Mater, 2001, 45: 1365–1371.
- [7] ZHU Zu-fang. The corrosion resistance and applications of coloured metals [M]. Beijing: Chemical Industry Press, 1995: 61. (in Chinese)
- [8] POLMEAR J. Magnesium alloys and applications [J]. Materials Science and Technology, 1994, 10: 1–16.
- [9] SHECHTMAN D, BLECH I, CRATIAS D. Metallic phase with long range orientational order and no translational symmetry [J]. Phys Rev Lett, 1984, 53: 1951–1953.
- [10] YI S, PARK E S, OK J B. (Icosahedral phase +  $\alpha$ -Mg) two phase microstructures in the Mg-Zn-Y ternary system [J]. Mater Sci Eng A, 2001, 300: 312–315.
- [11] SINGH A, SOMEKAWA H, MUKAI T. Compressive strength and yield asymmetry in extruded Mg-Zn-Ho alloys containing quasicrystal phase [J]. Scripta Mater, 2007, 56: 935–938.
- [12] XU D K, TANG W N, LIU L, XU Y B, HAN E H. Effect of Y concentration on the microstructure and mechanical properties of as-cast Mg-Zn-Y-Zr alloys [J]. Journal of Alloys and Compounds, 2007, 432: 129–134.
- [13] SHI Fei, GUO Xue-feng, ZHANG Zhong-ming. Quasicrystal of as-cast Mg-Zn-Y alloy [J]. The Chinese Journal of Nonferrous Metals, 2004, 14(1): 112–116. (in Chinese)
- [14] RUDD A L, BRESLIN C B, MANSFLED F. The corrosion protection afforded by rare earth conversion coatings applied to magnesium [J]. Corrosion Science, 2000, 42(2): 275–288.
- [15] KAWAMURA Y, HAYASHI K, INOUE A. Rapidly solidified powder metallurgy  $\text{Mg}_{97}\text{Zn}_1\text{Y}_2$  alloys with excellent tensile yield strength above 600 MPa [J]. Mater Trans, 2001, 42(7): 1172–1176.

(Edited by YANG Bing)